Isocyanurates with Planar Chirality: Design, Optical Resolution, and Isomerization

HIDETOSHI GOTO, MASANAO SUDOH, KEIKO KAWAMOTO, HIROSHI SUGIMOTO,* AND SHOHEI INOUE
Department of Industrial Chemistry, Faculty of Engineering, Tokyo University of Science, Tokyo, Japan

ABSTRACT Designs and syntheses of isocyanurates (**1–3**) are described on the basis of a novel concept that two enantiotopic faces of C_s-symmetric, prochiral planar molecules are differentiated with a location of groups at the top or bottom of the planar skeleton using a rigid linker. Such isocyanurates are atropisomeric. The planar-chiral structures of **1** and $\mathbf{2}_{anti}$ (*anti*-conformer of **2**) were confirmed by single-crystal X-ray analyses, and the space groups were $P1$ (for **1**) and $P2_1/c$ (for $\mathbf{2}_{anti}$), resulting that the crystals were racemates. Optical resolutions of **1–3** were successfully accomplished by using chiral high-performance liquid chromatography technique in combination with circular dichroism, absorption, and nuclear magnetic resonance spectroscopies and mass spectrometry. Furthermore, the rotational barriers ($\Delta G^{\ddagger}$s) related to isomerizations of **1–3** were estimated to be 27.2 (for **1** at 50 °C), 27.6 (for $\mathbf{2}_{anti}$ at 50 °C), and >40.6 (for $\mathbf{3}_{syn}$ at 150 °C) kcal/mol. The $\Delta G^{\ddagger}$s of **2** and **3** were higher than that of **1** and, in particular, that of **3** was highest among them. This result indicates that an introduction of bulky substituents and an intramolecular bridging are effective for inhibitions of the isomerizations. *Chirality 00:000–000, 2012.*

KEY WORDS: planar chirality; isocyanurate; atropisomerism; chiral resolution; racemization; isomerization; thermodynamics; kinetics

INTRODUCTION

Planar-chiral molecules have been developed from the aspect of not only unique three-dimensional structures[1–14] but also potential applications to auxiliaries and catalysts for asymmetric syntheses,[15–31] catalysts for stereospecific polymerizations,[32,33] and chiral sensors.[34,35] Our previous interests were focused on chiral porphyrins[36–62] having topological chiralities to provide model compounds of chiral porphinoids being abundant in living systems.[63–73] In particular, planar-chiral porphyrins[41,42,44,50–52] were found to work as effective chiral catalysts for asymmetric oxidations and as effective selectors for biomolecules. Among such planar-chiral porphyrins, we have paid attention to topological, chiral structures of *strapped* (or *fly-over*) porphyrins adopting cyclophane-type structures composed of planar porphyrin rings and flexible straps via covalent linkages.[50–56] Most recently, we designed planar-chiral metal complexes on the basis of our novel concept: planar structures built up of metal species and two metal-coordinating moieties via coordination bond may be employed as alternatives of planar porphyrin rings.[74] In fact, fly-over-type metal complexes consisting of square-planar-coordinated metals and achiral flexible tetradentate ligands were synthesized, and the optical resolutions of the racemic complexes were subsequently accomplished.[74]

In general, such planar-chiral molecules have been developed on the basis of design concepts as follows (Fig. 1). Achiral planar skeletons ($D_{\infty h}$-symmetry) are desymmetrized by attachment of substituent or functional groups to form prochiral planar skeletons (P) (C_s-symmetry) with enantiotopic planes; the orientations of the planes are indicated by arrow (Fig. 1A). As functional groups (Q) are located at the top or bottom of the prochiral planar skeletons (P) through covalent or coordination bonding, the molecules are planar-chiral (C_1-symmetric) (Fig. 1B). Metal (Q)-coordination perpendicular to the enantiotopic plane of P is one of the most widely used strategy; chiral metallocenes and π-arene complexes are representatives (Fig. 1C).[10–14,20–31] Bridging between P and Q with two flexible linkers (L^1s) generates cyclic molecules such as cyclophanes[1–9,15–19] and strapped porphyrins,[50–56] which is also one of the most widely used strategy (Fig. 1D). Herein, if a single rigid linker (L^2) is employed instead of the L^1s, the planar-chiral structure might be retained, which is our concept (Fig. 1E) (see footnote[1]). As the prochiral planar skeletons (Ps) in Figure 1D and E rotate around the bonds between P and L^1 or L^2, the planar-chiral compounds are

*Correspondence to: Hiroshi Sugimoto, Department of Industrial Chemistry, Faculty of Engineering, Tokyo University of Science, 12-1 Ichigaya-funagawara, Shinjuku, Tokyo 162-0826, Japan. E-mail: hrssgmt@rs.kagu.tus.ac.jp
Received for publication 13 April 2012; Accepted 06 June 2012
DOI: 10.1002/chir.22093
Published online in Wiley Online Library (wileyonlinelibrary.com).

[1]Both models of two compounds as shown in Figure 1D and E have two topological chiralities. One is planar chirality generated as the achiral desymmetrized planes (Ps) are marked from out-of-plane, substituent or functional groups (Q and L^1 or L^2). The other is axial chirality generated as the bonds between the planes (Ps) and the groups (L^1 or L^2) are focused on. During such chiralities, we have paid attention on the planar chirality in this report. This is due to two following points. First, the difference between our planar-chiral concept and axially chiral aromatic systems such as 1,1-binaphthol is the existence of the phenyl (Q) group connected to the phenylene (L^2) group. The bulky Q group covers the top or bottom of the isocyanurate (P) platform by the steric repulsion between the phenyl and isocyanurate rings. Secondly, our motivation is to develop analogs of planar-chiral porphinoids and to utilize the isocyanurate skeletons as the platform of the functional materials. In fact, in our laboratory, metalloporphyrins have frequently been employed not only as chiral catalysts for asymmetric syntheses and chiral selectors for biomolecules[36–62] but also as catalysts for precision macromolecular syntheses (polymethacrylates, polyesters, polyethers, polycarbonates, and so on).[118] In addition, we employed an isocyanurate skeleton as the platform for distinguishing enantiomers of guest molecules as described in the following sections. The isocyanurates had *flexible* amino acid units with central chirality.[96]

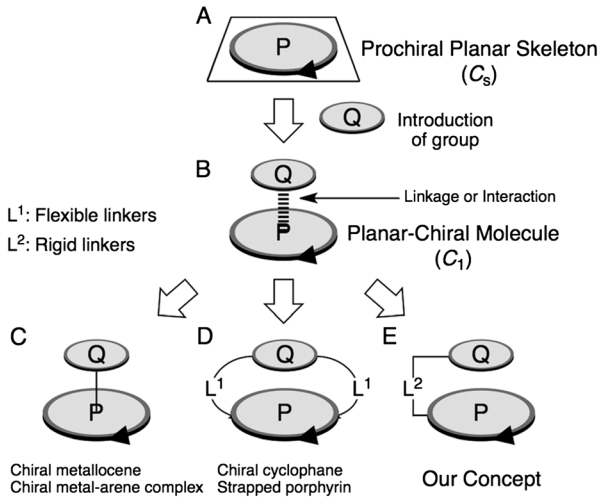

Fig. 1. Designs of planar-chiral molecules based on achiral planar skeletons. The planar skeletons ($D_{\infty h}$-symmetry) are desymmetrized by attachment of substituent or functional groups to form prochiral planar skeletons (P) (C_s-symmetry) with enantiotopic planes; the orientations of the planes are indicated by arrow (**A**). Planar-chiral molecules are generated by introduction of Q at the top or bottom of the enantiotopic plane of P through linkages or interactions (**B**). Chiral metal complexes using coordination bondings (**C**), chiral molecules using flexible covalent linkages (**D**), and planar-chiral molecules using rigid covalent linkages based on our concept (**E**).

isomerized (Fig. 2A and B). Because the atropisomerizations of the cyclophanes are prevented by bulky groups (Rs) introduced to P, the inhibition of the isomerizations of the conceptual, planar-chiral molecules might be accomplished in the similar way as well. Furthermore, the arrangement of two R units at equally neighboring positions of the bond between P and L^2 induces an orthogonal conformation of L^2–Q against P (Fig. 2B). Cyclic *N*-phenylimides adopt the orthogonal conformation due to steric repulsion between the ortho H atoms of the phenyl group and the O atoms (Fig. 2C).[75–77]

We have focused our interests on isocyanurate[78–95] for the purpose of the synthesis and utility of novel enzyme models

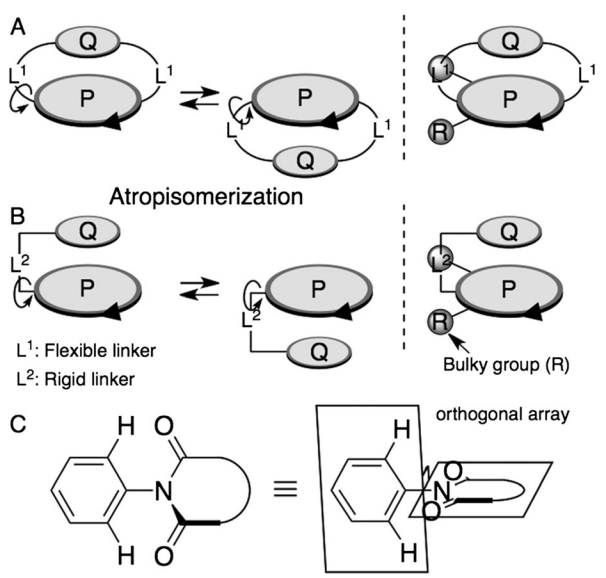

Fig. 2. Atropisomerization mechanisms of cyclophanes (**A**) and our conceptual planar-chiral molecules (**B**) and models of planar-chiral molecules bearing bulky groups (R) for inhibition of atropisomerization. (**C**) Conformation of *N*-phenyl-substituted cyclic imides.

because the isocyanurate framework is a rigid six-membered ring and has three O atoms with electron-donating properties and three N atoms to which a variety of functional groups is connected. Optically active isocyanurates having three flexible amino acid units were previously reported to distinguish between enantiomers of guest molecules.[96] In this study, a planar-chiral isocyanurate [1-(biphenyl-2-yl)-3-phenyl-1,3,5-triazinane-2,4,6-trione (**1**)] bearing phenyl and 2′-biphenyl groups at two N atoms of the isocyanurate backbone was designed (Fig. 3). Although the synthesis and optical resolution of **1** ahead of 1,3-bis(biphenyl-2-yl)-1,3,5-triazinane-2,4,6-trione (**2**) and *O*,*O*′-(hexane-1,6-diyl)-1-(3-oxybiphenyl-2-yl)-3-(2-oxyphenyl)-1,3,5-triazinane-2,4,6-trione (**3**) were accomplished, racemization of **1** proceeded at ambient temperature. Our ideas to suppress the atropisomerization of **1** were to introduce a bulky substituent (for **2**) and to intramolecularly bridge (for **3**). Racemization of **2** was slower than that of **1**, and no racemization of **3** was observed. The details will be described hereinafter.

MATERIALS AND METHODS

Materials

Dimethyl cyanocarbonimidodithioate, 2-phenylaniline, bromobenzene, BBr_3 (1 M in CH_2Cl_2), and 1,6-dibromohexane were purchased from Tokyo Chemical Industry (Tokyo, Japan). Isocyanatobenzene and 1-isocyanato-2-methoxybenzene were purchased from (Sigma-Aldrich (St. Louis, MO, USA). Trifluoroacetic acid was purchased from Wako Pure Chemical Industries (Osaka, Japan). Triethylamine (Et_3N) and 1,4-dioxane were dried with CaH_2 and then distilled over sodium benzophenone ketyl under nitrogen. Acetonitrile and CH_2Cl_2 were dried with CaH_2 and then distilled over CaH_2 under nitrogen. Isocyanatobenzene, 2-isocyanato-1,1′-biphenyl, 1-isocyanato-2-methoxybenzene, 1,6-dibromohexane, and bromobenzene were distilled under reduced pressure. Dimethyl cyanocarbonimidodithioate was recrystallized from toluene. Other reagents were used without purification. Compound **7**[97] and ethyl *N*-carbonylcarbamate[98] were synthesized by the literatures' methods.

Instruments

Hydrogen and carbon nuclear magnetic resonance (^1H and ^{13}C NMR) measurements were performed at 400 and 100 MHz with $CDCl_3$ or DMSO-d_6 as the solvents at 30 °C on a Bruker BioSpin DPX-400 spectrometer (Billerica, MA, USA). They were referenced using tetramethylsilane (TMS; δ 0.00) or the solvent residual signal as an internal standard. The chemical shift values are expressed as δ values (ppm), and the couple constants values (J) are in Hertz (Hz). The following abbreviations were used for signal multiplicities: s, singlet; d, doublet; t, triplet; dd, double-doublet; dt, double-triplet; m, multiplet; and br, broad. Infrared (IR) spectra were recorded using a JASCO FT/IR-4100 spectrometer (Hachioji, Japan). Electron spray ionization mass spectra were measured using a Bruker Daltonics microTOF-NR focus mass spectrometer. Absorption measurements were performed on a JASCO V-550 spectrometer. Circular dichroism (CD) measurements were carried out with a JASCO J-725 spectropolarimeter. Optical rotations were measured using a Horiba SEPA-200 polarimeter (Kyoto, Japan). Melting points were measured using a MEL-TEMP II melting point apparatus (Laboratory Devices, Holliston, MA, USA). Elemental analyses were performed by using a Perkin-Elmer 2400II

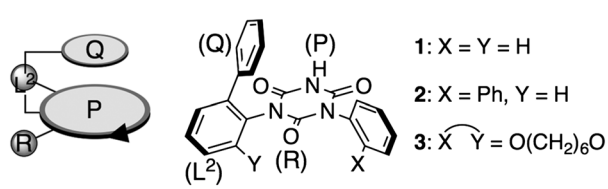

Fig. 3. Design concept and structures of planar-chiral isocyanurates (**1–3**).

CHN analyzer (Waltham, MA, USA). High-performance liquid chromatography (HPLC) experiments for estimations of enantiomeric excesses were carried out on a Hitachi instrument (L-7610 degasser, L-6000 pump, L-7400 UV detector, and D-2500 integrator) (Tokyo, Japan) with a Sumichiral® OA-4600 [25 × 0.46 (i.d.) cm, 5 μm particle; Sumika Chemical Analysis Service, Tokyo, Japan]. HPLC experiments for separations and isolations of stereoisomers were performed on a Hitachi instrument (L-7110 pump, L-7250 autosampler, L-4000 H UV detector, L-5200 fraction collector, and D-2500 integrator) with a Sumichiral® OA-4600 [25 × 2 (i.d.) cm, 5 μm particle]. Single crystal X-ray analyses were conducted using a Bruker AXS SMART X-ray diffractometer equipped with a CCD area director and Mo-K_α radiation (λ = 0.71073 Å).

Synthesis of Isocyanurate 1

Methyl *N*-(biphenyl-2-yl)-*N*′-cyanoimidothiocarbamate (4)[99]. A solution of dimethyl cyanocarbonimidodithioate (73.1 g, 500 mmol) purified by recrystallization and 2-phenylaniline (84.6 g, 500 mmol) in ethanol (500 ml) was heated under reflux. The color of the solution gradually changed from slight yellow to brown during heating. After being heated for 11 days, the mixture was cooled to room temperature. The mixture was concentrated under high vacuum to leave a crude product as a white powder. The product was purified by recrystallization from ethanol to afford **4** as a slightly yellow needle crystal (27.6 g, 103 mmol, 20.6%). mp: 166.8–168.5 °C. ^{1}H NMR ($CDCl_3$): δ 2.31 (s, 3H, C*H*$_3$), 7.34 (d, *J* = 6.4 Hz, 2H, Ar–*H*), 7.37–7.45 (m, 5H, Ar–*H*), 7.48 (t, *J* = 6.4 Hz, 2H, Ar–*H*), 7.66 (br, 1H, N*H*). ^{13}C NMR ($CDCl_3$): δ 14.56, 114.51, 127.15, 128.41, 128.57, 129.03, 129.09, 130.95, 132.98, 137.48. IR (KBr, cm^{-1}): 3198 ($\nu_{N\text{-}H}$), 2170 ($\nu_{C\equiv N}$), 1524 (ν_{CN}).

1-[5-(Biphenyl-2-yl)-4-(methylthio)-6-oxo-1-phenyl-5,6-dihydro-1,3,5-triazin-2(1*H*)-ylidene]-3-phenylurea (5)[99]. After Et_3N (1.14 ml, 8.36 mmol) was added to a white suspension of **4** (2.14 g, 8.00 mmol) in acetonitrile (24 ml under nitrogen), the mixture was heated at 60 °C for 30 min. Isocyanatobenzene (1.74 ml, 16.0 mmol) was dropwise added to the suspension at 60 °C over 10 min. The white suspension became a slightly yellow solution during the dropwise addition. After being stirred at 60 °C for 4 h, the reaction mixture was cooled to room temperature. The mixture was concentrated under high vacuum to leave a crude product as a yellow powder. The product was purified by recrystallization from $CHCl_3$/hexane twice to afford **5** as a white powder (3.90 g, 7.72 mmol, 96.5%). mp: 215.3–217.1 °C. ^{1}H NMR ($CDCl_3$): δ 2.38 (s, 3H, C*H*$_3$), 6.78 (s, 1H, N*H*), 7.01 (t, *J* = 7.2 Hz, 1H, Ar–*H*), 7.13 (d, *J* = 7.2 Hz, 2H, Ar–*H*), 7.25 (t, *J* = 7.2 Hz, 2H, Ar–*H*), 7.31–7.48 (m, 12H, Ar–*H*), 7.50 (dt, *J* = 7.6 and 1.2 Hz, 1H, Ar–*H*), 7.59 (dt, *J* = 7.6 and 1.2 Hz, 1H, Ar–*H*). ^{13}C NMR ($CDCl_3$): δ 15.56, 119.35, 123.39, 128.34, 128.44, 128.57, 128.66, 128.92, 128.95, 129.04, 129.55, 129.87, 131.17, 131.68, 131.70, 135.13, 137.79, 138.75, 142.14, 149.10, 167.63. IR (KBr, cm^{-1}): 3407 ($\nu_{N\text{-}H}$), 1731 (ν_{CO}), 1682 (ν_{CO}), 1636 ($\nu_{C\text{-}N}$), 1511 (ν_{CN}).

1-(Biphenyl-2-yl)-3-phenyl-1,3,5-triazinane-2,4,6-trione (1)[99]. When an HCl aqueous solution (2 M, 50 ml, 100 mmol) was added to a solution of **5** (1.77 g, 3.50 mmol) in 1,4-dioxane (35 ml), the mixture gradually became turbid. During heating of the white suspension, the suspension gradually changed to the colorless clear solution. After being heated under reflux for 90 min, the reaction mixture was cooled to room temperature and further stored in a refrigerator (~ 5 °C) for 10 days to leave a crude product as a white powder. The product was purified by recrystallization from $CHCl_3$/hexane twice to afford **1** as a white powder (0.843 g, 2.36 mmol, 67.6%). mp: 212.0–212.5 °C. ^{1}H NMR ($CDCl_3$): δ 6.98 (br, 2H, Ar–*H*), 7.26–7.32 (m, 2H, Ar–*H*), 7.37 (dd, *J* = 7.6 and 1.6 Hz, 1H, Ar–*H*), 7.39–7.47 (m, 7H, Ar–*H*), 7.49 (dt, *J* = 8.0 and 2.0 Hz, 1H, Ar–*H*), 7.54 (dt, *J* = 7.2 and 1.6 Hz, 1H, Ar–*H*), 8.37 (br, 1H, N*H*). ^{13}C NMR ($CDCl_3$/CD_3OD = 9/1, v/v): δ 127.91, 128.20, 128.27, 128.39, 128.66, 129.09, 129.28, 129.35, 129.86, 130.79, 131.16, 133.02, 138.28, 141.33, 148.41, 148.58, 149.37 135.13, 137.79, 138.75, 142.14, 149.10, 167.63. IR (KBr, cm^{-1}): 3212 ($\nu_{N\text{-}H}$), 1718 (ν_{CO}), 1693 (ν_{CO}). HRMS–ESI (*m*/*z*): $[M - H]^-$calcd for $C_{21}H_{14}N_3O_3$, 356.1035; found, 356.1039. Anal. Calcd for $C_{21}H_{15}N_3O_3 \cdot 0.2H_2O$: C, 69.88; H, 4.30; N, 11.64. Found: C, 69.81; H, 3.99; N, 11.64. Crystallographic data for the structure of **1** have been deposited with the Cambridge Crystallographic Data Centre (CCDC-857457). Copies of the data can be obtained, free of charge, on application to the Director, CCDC, 12 Union Road, Cambridge CB2 1EZ, United Kingdom (Fax: 44-1223-336033 or E-mail: deposit@ccdc.cam.ac.uk).

Synthesis of Isocyanurate 2

1-[1,5-Bis(biphenyl-2-yl)-4-(methylthio)-6-oxo-5,6-dihydro-1,3,5-triazin-2(1*H*)-ylidene]-3-phenylurea (6)[99]. After Et_3N (8.5 ml, 60 mmol) was added to a white suspension of **4** (13.0 g, 48.4 mmol) in acetonitrile (170 ml under nitrogen), the mixture was heated at 40 °C for 30 min. 2-Isocyanato-1,1′-biphenyl (17.6 ml, 102 mmol) was dropwise added to the suspension at 60 °C over 10 min. The white suspension became a colorless clear solution during the dropwise addition. When heated at 60 °C for approximately 1 h, the mixture gradually changed to a white suspension powder. After heating the suspension at 60 °C for 24 h, the precipitate was collected by suction filtration and washed with acetonitrile to afford **6** as a white powder. The filtrate was concentrated under high vacuum to leave a crude product as a white powder. The crude product was purified by silica gel chromatography with $CHCl_3$/acetone (15/1, v/v) and subsequent recrystallization from $CHCl_3$/hexane twice to obtain **6** as a white powder (total yield: 16.0 g, 24.3 mmol, 50.1%). mp: 172.7–175.2 °C (dec). ^{1}H NMR ($CDCl_3$): δ 2.29 (s, 3H, C*H*$_3$), 6.29 (s, 1H, N*H*), 6.91 (d, *J* = 7.6 Hz, 1H, Ar–*H*), 6.95 (dd, *J* = 7.6 and 1.6Hz, 1 H, Ar–*H*), 6.99–7.18 (m, 6H, Ar–*H*), 7.22 (dd, *J* = 7.6 and 1.6 Hz, 1H, Ar–*H*), 7.26–7.35 (m, 4H, Ar–*H*), 7.36–7.48 (m, 12H, Ar–*H*), 7.55 (dt, *J* = 7.6 and 1.2 Hz, 1H, Ar–*H*), 8.05 (br, 1H, Ar–*H*). ^{13}C NMR ($CDCl_3$): δ 15.46, 123.84, 124.62, 127.17, 127.77, 128.15, 128.20, 128.26, 128.46, 128.55, 128.59, 128.72, 128.83, 128.87, 128.98, 129.17, 129.23, 129.51, 129.66, 129.90, 130.31, 130.43, 130.83, 131.02, 131.71, 132.04, 132.23, 132.86, 134.70, 138.13, 138.53, 139.13, 140.03, 142.61, 146.53, 149.54, 160.18, 167.08. IR (KBr, cm^{-1}): 3394 ($\nu_{N\text{-}H}$), 1734 (ν_{CO}), 1693 (ν_{CO}), 1638 ($\nu_{N\text{-}H}$), 1505 (ν_{CN}).

1,3-Bis(biphenyl-2-yl)-1,3,5-triazinane-2,4,6-trione (2)[99]. After **6** (16.0 g, 24.3 mmol) was dissolved in 1,4-dioxane (320 ml) under reflux, an HCl aqueous solution (2 M, 450 ml, 900 mmol) was added to the solution. After being heated under reflux for 2.5 h, the mixture was cooled to room temperature. The mixture was concentrated under high vacuum to leave a crude product as a yellow solid. The product was purified by silica gel chromatography with $CHCl_3$/acetone (15/1, v/v) and subsequent recrystallization from benzene twice to afford **2** as a white solid (total yield: 2.52 g, 5.88 mmol, 24.2%). mp: 224.8–226.1 °C. ^{1}H NMR ($CDCl_3$): δ 6.91 (dd, *J* = 7.6 and 1.2 Hz, 2H, Ar–*H*), 7.22–7.29 (m, 6H, Ar–*H*), 7.37–7.46 (m, 10H, Ar–*H*), 7.49 (dt, *J* = 7.6 and 1.6 Hz, 2H, Ar–*H*), 7.63 (br, 1H, N*H*). ^{13}C NMR ($CDCl_3$): δ 128.10, 128.38, 128.48, 128.55, 128.89, 130.10, 130.94, 130.96, 138.31, 141.51, 147.59, 148.88. IR (KBr, cm^{-1}): 3209 ($\nu_{N\text{-}H}$), 1727 (ν_{CO}), 1698 (ν_{CO}). HRMS–ESI (*m*/*z*): $[M - H]^-$calcd for $C_{27}H_{18}N_3O_3$, 432.1348; found, 432.1346. Anal. Calcd for $C_{27}H_{19}N_3O_3 \cdot 0.1H_2O$: C, 74.50; H, 4.45; N, 9.65. Found: C, 74.40; H, 4.25; N, 9.64. Crystallographic data for the structure of $\mathbf{2}_{anti}$ have been deposited with the Cambridge Crystallographic Data Centre (CCDC-857458). Copies of the data can be obtained, free of charge, on application to the Director, CCDC, 12 Union Road, Cambridge CB2 1EZ, United Kingdom (Fax: 44-1223-336033 or E-mail: deposit@ccdc.cam.ac.uk).

Synthesis of Isocyanurate 3

1-Methoxy-6-phenylaniline (8). NaOH (2.23 g, 55.8 mmol, pellet) was added to a solution of *N*-(3-methoxybiphenyl-2-yl)acetamide (**7**)[97] (2.71 g, 11.2 mmol) in ethanol (100 ml). After being heated under reflux for 8 days, the reaction mixture was cooled to room temperature. The mixture was concentrated under high vacuum to leave a residue as a viscous brown liquid. A solution of the residue in $CHCl_3$ was washed with water, dried over Na_2SO_4, and concentrated by rotary evaporator to leave a crude product as a viscous brown liquid. The product was purified by silica gel chromatography with hexane/ethyl acetate (1/1, v/v) to afford **8** as a brown liquid (1.98 g, 9.94 mmol, 88.7%). ^{1}H NMR ($CDCl_3$): δ 3.82 (s, 3H, OC*H*$_3$), 4.28 (br, 2H, N*H*$_2$), 6.64–7.47 (m, 8H, Ar–*H*). MS–ESI (*m*/*z*): 201.10 $[M + Na]^+$.

1-(3-Methoxybiphenyl-2-yl)-3-(2-methoxyphenyl)urea (9). 1-Isocyanato-2-methoxybenzene (1.2 ml, 9.5 mmol) was dropwise added to a mixture of **8** (1.90 g, 9.54 mmol) and Et_3N (0.3 ml, 2.2 mmol) in 1,4-dioxane (30 ml) at room temperature over 10 min under nitrogen. During stirring of the mixture at 35 °C, the color of the solution gradually changed from slight yellow to brown. After stirring the mixture for 4.5 h, the conversion of **8** was approximately 30%. 1-Isocyanato-2-methoxybenzene (4.0 ml, 30 mmol) was further added to the mixture. After being stirred at 35 °C for further 4 h, the mixture was cooled to room temperature. Ethanol was added to the mixture to quench an excess amount of the isocyanate. The mixture was concentrated under high vacuum to leave a crude product as a dark brown viscous oil. The product was purified by silica gel chromatography with $CHCl_3$/methanol (10/1, v/v) to afford **9** as a white powder (1.34 g, 3.68 mmol, 38.5%). mp: 166.2–167.5 °C. ^{1}H NMR (DMSO-d_6): δ 3.81 (s, 3H, OCH_3), 3.81 (s, 3H, OCH_3), 6.80 (dt, J = 7.6 and 1.6 Hz, 1H, Ar–*H*), 6.86 (dt, J = 7.6 and 1.6 Hz, 1H, Ar–*H*), 6.92 (dd, J = 8.0 and 1.6 Hz, 1H, Ar–*H*), 6.95 (dd, J = 8.0 and 1.6 Hz, 1H, Ar–*H*), 7.07 (dd, J = 8.0 and 1.2 Hz, 1H, Ar–*H*), 7.25–7.34 (m, 2H, Ar–*H*), 7.34–7.42 (m, 4H, Ar–*H*), 7.97 (dd, J = 8.0 and 1.6 Hz, 1H, Ar–*H*), 8.02 (br, 1H, N*H*), 8.10 (s, 1H, N*H*). ^{13}C NMR ($CDCl_3$): δ 55.71, 56.06, 110.04, 110.80, 119.24, 121.27, 122.33, 122.95, 123.57, 127.65, 128.00, 128.51, 128.67, 129.05, 138.83, 140.88, 147.90, 154.22, 155.27. IR (KBr, cm^{-1}): 3320 ($\nu_{N\text{-}H}$), 1649 (ν_{CO}), 1543 ($\nu_{N\text{-}H}$), 1256 ($\nu_{C\text{-}O\text{-}C}$). MS–ESI (*m*/*z*): 349.14 $[M + H]^+$.

1-(3-Hydroxybiphenyl-2-yl)-3-(2-hydroxyphenyl)urea (10). BBr_3 (1 M in CH_2Cl_2, 50 ml, 50 mmol) was dropwise added to a solution of **9** (1.20 g, 3.29 mmol) in CH_2Cl_2 (300 ml) at 0 °C over 4 h under nitrogen. During stirring of the solution at room temperature, the color of the solution gradually changed from colorless to gray. After being stirred for 18 h, the mixture was carefully poured into water (200 ml) to quench an excess amount of BBr_3. During quenching, a large amount of a white powder appeared in the mixture. The precipitate was collected by suction filtration, washed with water, and dried in vacuo to afford **10** as a white powder (1.04 g, 3.25 mmol, 98.7%). mp: 152.6–154.5 °C (dec.). ^{1}H NMR (DMSO-d_6): δ 6.68 (dt, J = 7.2 and 1.6 Hz, 1H, Ar–*H*), 6.74 (dt, J = 7.6 and 1.6 Hz, 1H, Ar–*H*), 6.77 (dd, J = 8.0 and 1.6 Hz, 1H, Ar–*H*), 6.78 (dd, J = 8.0 and 1.6 Hz, 1H, Ar–*H*), 6.90 (dd, J = 8.0 and 1.6 Hz, 1H, Ar–*H*), 7.14 (t, J = 8.0 Hz, 1H, Ar–*H*), 7.27–7.34 (m, 1H, Ar–*H*), 7.39 (d, J = 8.0 Hz, 4H, Ar–*H*), 7.86 (dd, J = 8.0 and 1.6 Hz, 1H, Ar–*H*), 8.12 (br, 2H, N*H*) 9.44 (br, 1H, O*H*), 9.75 (s, 1H, O*H*). ^{13}C NMR (DMSO-d_6): δ 114.58, 115.64, 118.60, 119.08, 120.79, 121.55, 122.96, 126.84, 126.90, 128.10, 128.71, 139.77, 140.22, 145.50, 153.56, 154.46. IR (KBr, cm^{-1}): 3467 ($\nu_{O\text{-}H}$), 3288 ($\nu_{N\text{-}H}$), 1627 (ν_{CO}), 1559 ($\nu_{N\text{-}H}$), 1102 ($\nu_{C\text{-}OH}$). MS–ESI (*m*/*z*): 343.12 $[M + Na]^+$.

***O,O′*-(Hexane-1,6-diyl)-1-(3-oxybiphenyl-2-yl)-3-(2-oxyphenyl) urea (11)**. 1,6-Dibromohexane (0.50 ml, 3.3 mmol) was added to a suspension of **10** (1.05 g, 3.27 mmol) and K_2CO_3 (3.0 g, 22 mmol) in acetonitrile (1.5 l) at 0 °C under nitrogen, and the mixture was then stirred at room temperature. After stirring the mixture for 7 days, the conversion of **10** was approximately 30%. After the mixture was stirred at 35 °C for further 14 days, the conversion of **10** was over 90%. The color of the supernatant gradually changed from colorless to yellow during stirring. After cooled to room temperature, the mixture was concentrated under high vacuum to leave a yellow solid. After the solid was dissolved in a mixture of $CHCl_3$/water, the organic solution was collected by a separating funnel, washed with water, and dried over Na_2SO_4 to leave a crude product as a slightly yellow solid. The product was purified by silica gel chromatography with $CHCl_3$/ethyl acetate (9/1, v/v) to afford **11** as a white solid (0.623 g, 1.55 mmol, 47.4%). mp: 219.7–223.4 °C (dec.). ^{1}H NMR (DMSO-d_6): δ 1.57 (br, 2H, CH_2), 1.67 (br, 6H, CH_2), 3.96 (br, 2H, OCH_2), 4.15 (br, 2H, OCH_2), 6.85 (dt, J = 7.6 and 1.6 Hz, 1H, Ar–*H*), 6.96 (dd, J = 7.6 and 1.2 Hz, 1H, Ar–*H*), 6.98 (dd, J = 8.0 and 1.6 Hz, 1H, Ar–*H*), 7.00 (dt, J = 8.0 and 1.6 Hz, 1H, Ar–*H*), 7.07 (dd, J = 7.2 and 1.2 Hz, 1H, Ar–*H*), 7.29 (d, J = 8.0 Hz, 1H, Ar–*H*), 7.34 (dt, J = 8.0 and 1.2 Hz, 2H, Ar–*H*), 7.43 (t, J = 7.6 Hz, 2H, Ar–*H*), 7.51 (dd, J = 8.0 and 1.2 Hz, 1H, Ar–*H*), 7.69 (br, 1H, N*H*), 7.85 (br, 1H, N*H*). ^{13}C NMR (DMSO-d_6): δ 26.53, 27.58, 28.59, 29.48, 69.56, 70.77, 113.20, 113.40, 120.39, 122.23, 123.35, 123.66, 125.61, 126.98, 127.63, 127.95, 128.06, 128.77, 128.88, 129.00, 139.61, 142.09, 149.38, 155.78, 156.17. IR (KBr, cm^{-1}): 3323 ($\nu_{N\text{-}H}$), 1650 (ν_{CO}), 1549 ($\nu_{N\text{-}H}$), 1242 ($\nu_{C\text{-}O\text{-}C}$). MS–ESI (*m*/*z*): 425.18 $[M + Na]^+$.

***O,O′*-(Hexane-1,6-diyl)-1-(3-oxybiphenyl-2-yl)-3-(2-oxyphenyl)-1,3,5-triazinane-2,4,6-trione (3)**[100,101]. Ethyl *N*-carbonylcarbamate[98] (1.35 ml, 1.31 mmol) was added to a suspension of **11** (0.533 g, 1.33 mmol) in dry bromobenzene (60 ml) at room temperature under nitrogen. During heating of the mixture under reflux, the suspension became a slightly brown solution during heating. After being heated under reflux for 24 h, the mixture was cooled to room temperature. The mixture was concentrated under high vacuum to leave a crude product as a slightly brown viscous liquid. The product was purified by silica gel chromatography with $CHCl_3$/acetone (30/1 to 10/1, v/v) and subsequent reprecipitation with $CHCl_3$/hexane to afford **3** as a white solid (0.152 g, 0.322 mmol, 24.2%). mp: 286.4–288.2 °C. ^{1}H NMR ($CDCl_3$): δ 1.47–1.67 (m, 4H, CH_2), 1.71 (br, 2H, CH_2), 1.81 (br, 2H, CH_2), 3.90 (dt, J = 9.2 and 1.6 Hz, 1H, OCH_2), 3.99 (dt, J = 9.2 and 1.6 Hz, 1H, OCH_2), 4.19 (m, 2H, OCH_2), 6.91 (dd, J = 8.0 and 2.0 Hz, 1H, Ar–*H*), 6.97 (d, J = 7.2 Hz, 1H, Ar–*H*), 6.98 (dd, J = 8.0 and 1.6 Hz, 1H, Ar–*H*), 7.01 (t, J = 8.0 Hz, 2H, Ar–*H*), 7.26–7.40 (m, 6H, Ar–*H*), 7.43 (t, J = 8.0 Hz, 1H, Ar–*H*), 8.21 (s, 1H, N*H*). ^{13}C NMR ($CDCl_3$): δ 27.72, 27.84, 29.07, 29.19, 69.08, 70.04, 112.65, 113.67, 120.61, 121.21, 122.40, 122.50, 127.99, 128.33, 128.37, 129.69, 130.75, 131.16, 138.30, 143.10, 147.70, 147.81, 148.54, 154.78, 154.96. IR (KBr, cm^{-1}): 3225 ($\nu_{N\text{-}H}$), 1723 (ν_{CO}), 1700 (ν_{CO}), 1291 ($\nu_{C\text{-}O\text{-}C}$). HRMS–ESI (*m*/*z*): $[M - H]^-$calcd for $C_{27}H_{24}N_3O_5$, 470.1716; found, 470.1708. Anal. Calcd for $C_{27}H_{25}N_3O_5 \cdot 0.4H_2O$: C, 67.74; H, 5.43; N, 8.78. Found: C, 67.71; H, 5.23; N, 8.74.

Optical Resolutions

A typical procedure for optical resolutions of **1–3** is described as follows. A stock solution (0.5 mg/ml) of **1** in a mixture of hexane/ethanol (9/1, v/v) including mesitylene (t_0 = 8.9 min) as a standard was prepared. A 1.5 ml aliquot of the **1** solution was injected into an HPLC system [eluent, hexane/ethanol/trifluoroacetic acid (90/10/0.5, v/v/v); flow speed: 6.5 ml/min] with a Sumichiral® OA-4600 [25 × 2 (i.d.) cm] to collect fractions. The solvents of the fractions were removed under reduced pressure at low temperature (less than 20 °C). The same operations were repeatedly carried out 10 times to give enantiometically pure **1a** (the first eluent) and **1b** (the second eluent) as white powders. The optical purities of the collected fractions were estimated to be more than 98% ee by the HPLC analyses.

Optical resolutions of **2** and **3** were also carried out under the same conditions except for initial concentrations of stock solutions [1.0 (for **2**) and 0.5 (for **3**) mg/ml]. Both chromatograms showed three peaks (10.9, 13.0, 19.6 min for **2** and 17.9, 19.6, 22.0 min for **3**), so all three components (**2a**, **2b**, **2c** for **2** and **3a**, **3b**, **3c** for **3**) were fractionated.

To measure optical rotations of the isolated stereoisomers of **1–3**, each stock solution of the isocyanurates in THF [10 mg/3 ml (= 0.333 g/dl)] was prepared by using measuring flasks. Each stock solution was transferred to a 1.0 cm quartz cell by a pipet (approximately 2 ml). Optical rotation measurements of the isomers were performed at ambient temperature (27–29 °C); **1a** [(−)-**1**]: $[\alpha]_D^{29}$ −116 (*c* 0.333, THF) (α −0.0384), **1b** [(+)-**1**]: $[\alpha]_D^{29}$ +120 (*c* 0.333, THF) (α +0.0399), **2a** [(−)-$\mathbf{2}_{anti}$]: $[\alpha]_D^{28}$ −141 (*c* 0.333, THF) (α −0.0468), **2b** [(+)-$\mathbf{2}_{anti}$]: $[\alpha]_D^{27}$ +146 (*c* 0.333, THF) (α +0.0485), **3a** [(−)-$\mathbf{3}_{syn}$]: $[\alpha]_D^{29}$ −126 (*c* 0.333, THF) (α −0.0420), **3b** [(+)-$\mathbf{3}_{syn}$]: $[\alpha]_D^{29}$ +127 (*c* 0.333, THF) (α +0.0424).

Absorption and Circular Dichroism Measurements

To measure absorption and CD spectra of the isolated stereoisomers of **1–3**, each stock solution of the isocyanurates in THF [6.3 mg/100 ml (0.18 mM for **1** s, 0.14 mM for **2** s, 0.13 mM for **3** s)] was prepared by using measuring flasks. Each stock solution was transferred to a 0.1-cm quartz cell by a pipet (approximately 0.5 ml). Absorption and CD spectra of the stereoisomers of the isocyanurates were measured at the ranges of 200–600 (for absorption) and 210–350 (for CD) nm at room temperature (25–27 °C).

Isomerization Investigations

A typical procedure for the investigations of the isomerizations of the isolated stereoisomers of the isocyanurates is described as follows. The solution (0.5 mg/ml) of **1a** in a mixture of hexane/ethanol (9/1, v/v) was prepared and then kept at 50 °C for a predetermined amount of time. At each predetermined time, a 100 µl aliquot of the solution was injected into the chiral HPLC system to estimate a stereoisomeric population of **1**. The stereoisomeric populations were plotted versus time, and then, an initial rate constant (k_T) of isomerization was calculated. Furthermore, the isomerization barrier ($\Delta G^{\ddagger}$) of **1** was calculated by using k_T and Eyring equation: $\Delta G_T^{\ddagger} = -RT \ln(k_T h/\kappa k_B T)$, where R is the universal gas constant (8.31441 J K/mol), T the absolute temperature (K), k_T the kinetic rate constant, h the Plank's constant (6.626176×10^{-34} J s), κ the transition factor ($\kappa = 0.5$), and k_B the Boltzmann constant (1.380662×10^{-23} J/K).[102–105]

The isomerization investigations of **2** and **3** were also carried out under the same conditions except for initial concentrations of stock solutions (1.0 (for **2**) and 0.5 (for **3**) mg/ml).

RESULT AND DISCUSSION

Synthesis and Characterization of 1

The synthesis of **1** was performed at three steps according to a method employed for a synthesis of an isocyanurate having two phenyl groups at two N atoms (Scheme 1).[99] 2-Phenylaniline as a starting material was reacted with dimethyl cyanocarbonimidodithioate under an equimolar condition in ethanol to afford methyl *N*-(biphenyl-2-yl)-*N*′-cyanoimidothiocarbamate (**4**). A condensation of **4** with two equivalents of isocyanatobenzene in acetonitrile containing Et_3N formed a corresponding triazine derivative, 1-[5-(biphenyl-2-yl)-4-(methylthio)-6-oxo-1-phenyl-5,6-dihydro-1,3,5-triazin-2(1*H*)-ylidene]-3-phenylurea (**5**). **5** was hydrolyzed under an acidic condition with aqueous HCl to obtain **1**.

For the purpose of investigating whether **1** forms a chiral conformation as expected, the characterization of **1** was carried out by using single crystal X-ray crystallography. Single crystals of **1** suitable for X-ray crystallographic analysis were obtained from the solution of **1** in a mixture of hexane/$CHCl_3$. The ball-and-stick drawing and packing of the crystal structure of **1** are drawn in Figs. 4 and S1 in the Supporting Information, respectively. The selected dihedral angles and lengths are summarized in Table 1. As three phenyl and one isocyanurate rings of **1** are denoted as Ph^1 (for the *N*-phenyl group), Ph^2 (for the phenylene group in

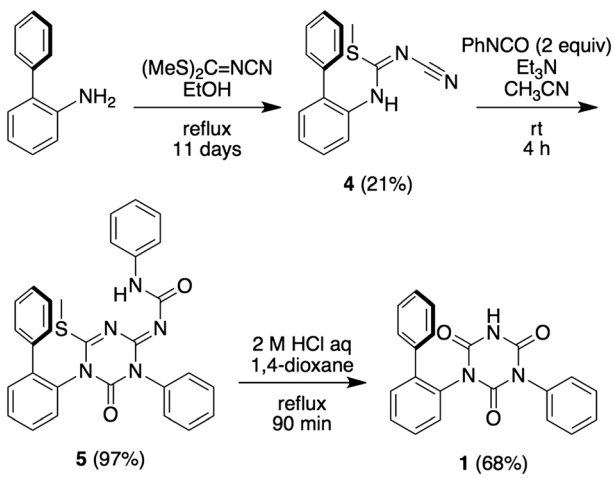

Scheme 1. Synthesis of **1**.

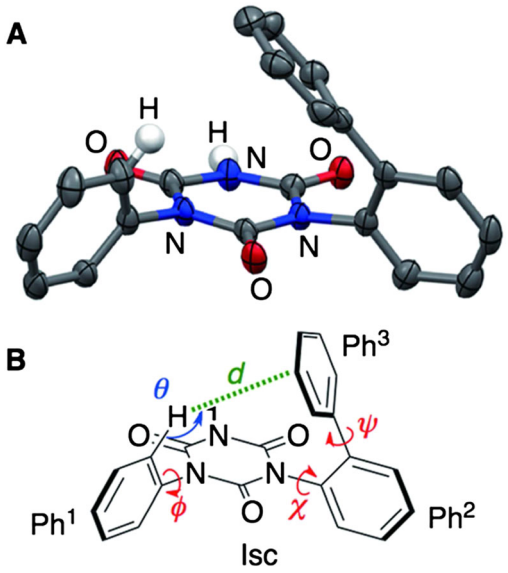

Fig. 4. (**A**) Ball-and-stick drawing of **1** with thermal ellipsoids at 50% probability. Each one of the independent molecules is shown here. H atoms are partially omitted for clarity. (**B**) Steric illustration of **1** with denotation of benzene and heterocyclic rings, dihedral angles, spatial distance, and angle: Ph^1, Ph^2, Ph^3 for three benzene rings; Isc for isocyanurate ring; ϕ, χ, ψ for three dihedral angles; d for spatial distance between carbon of Ph^3 and hydrogen at ortho position of Ph^1; for angle of C-H(Ph^1)···C(Ph^3).

TABLE 1. Selected structural data of 1

Dihedral angle (°)			Distance (Å)	Angle (°)
ϕ (Isc–Ph^1)	χ (Isc–Ph^2)	ψ (Ph^2–Ph^3)	d ($H^1_{Ph}\cdots C^3_{Ph}$)	θ (C-$H^1_{Ph}\cdots C^3_{Ph}$)
94.1	80.3	74.5	3.28	137.3
95.7	77.2	61.7	3.32	148.8
74.9	82.0	56.4	3.10	177.0
Mean 88.3	Mean 79.8	Mean 64.2	Mean 3.23	

N-(biphenyl-2-yl) one), Ph^3 (for the phenyl group in *N*-(biphenyl-2-yl) one), and Isc (for the isocyanurate skeleton), *vide infra*, three dihedral angles between two rings, a shortest spatial distance between C atoms of Ph^3 and an H atom at ortho position of Ph^1, an angle with the hydrogen as the center of C–H···C are represented as ϕ(Isc–Ph^1), χ(Isc–Ph^2), ψ(Ph^2–Ph^3), d($H^1_{Ph}\cdots C^3_{Ph}$), (C-$H^1_{Ph}\cdots C^3_{Ph}$) (Fig. 4B). **1** was crystallized in a triclinic system with a space group of *P*1. Six independent molecules, which are *pR*- and *pS*-forms of three different conformers, were found in the dissymmetric unit. The two phenyl groups (Ph^1 and Ph^2) covalently bonded to the imide N atoms were orthogonally distorted to the isocynanurate planes in the ranges of 74.9–95.7° for ϕ and 77.2–81.9° for χ because of steric repulsions between the phenyl rings and the oxygens on the isocyanurate ring. These values were comparable with torsion angles (60–80°) between benzene rings and heterocyclic rings of *N*,*N*′,*N*″-triphenylisocyanurates in crystal.[76,77] The dihedral angles (ψ) between Ph^2 and Ph^3 were 56.4–74.5° which are larger than those (~ 50°) between two benzene rings of ortho-terphenyl in crystal.[106–108] Furthermore, the spatial distances (ds) between the carbons of Ph^3s and the hydrogens

at ortho positions of Ph[1]s were 3.10–3.32 Å, being longer than those between hydrogens and aromatic rings in molecular structures formed by C-H···π-arene interactions.[109–111] These results suggest that **1** expectedly adopts a chiral conformation (C_1, centrosymmetric) stabilized by steric repulsion as the major driving force and CH–π interaction as the minor one in crystal. However, any crystals consisted of 1:1 mixtures of the antipodes.

Optical Resolution and Isomerization of 1

The optical resolution of **1** was carried out by using HPLC with Sumichiral® OA-4600 as a chiral column [eluent: hexane/ethanol/trifluoroacetic acid (90/10/0.5, v/v/v)] (Fig. 5). A chromatogram of **1** showed two peaks with comparable peak areas in 27.9 and 29.6 min (t_0 = 8.9 min for mesitylene as a standard material). Thus, **1** was fractionated to afford the components corresponding to the two peaks. Absorption (Fig. 6, bottom), ^{1}H NMR, and MS spectra of the component of the first fraction separated by chiral HPLC were identical with those of the second fraction. On the other hand, a CD spectrum of the component of the first fraction (**1a**) exhibited a negative Cotton effect at 230 nm, whereas that of the second fraction (**1b**) showed a positive Cotton effect. These CD patterns were completely mirror images in the range of 210–280 nm (Fig. 6, top). Furthermore, the optical rotations, $[\alpha]_D$s, of **1a** and **1b** were estimated to be −116 and +120, respectively. These results indicate that the two components (**1a** and **1b**) are a pair of enantiomers of **1** [**1a** = (−)-**1** and **1b** = (+)-**1**].

To investigate a thermal stability of **1** in solution, the change of the chromatogram of **1** was periodically monitored by chiral HPLC after the solutions of **1b** (98.5% ee) in hexane/ethanol (9/1, v/v) was kept at 50 °C for a predetermined amount of time. The peak of the chromatogram for **1b** gradually became lower over time, whereas that for **1a** became higher (Fig. 7). No other peaks were observed during incubation of the solution. Furthermore, the ^{1}H NMR spectra of the solutions before and after incubation were completely identical. These results suggest that racemization of **1** proceeded under the condition. The ratios of the **1b** area to the area of all peaks, that is [area of **1b**] / [[area of **1a**] + [area of **1b**]], were plotted with time in Figure 7. The first-order kinetic constant (k_{323}) and the half-life period [$\tau_{1/2(323)}$] of racemization at 50 °C (black circles) were estimated to be 2.86×10^{-6} sec^{-1} and 33.7 h (1.40 day), respectively. In addition, the Gibbs' free-energy change ($\Delta G^{\ddagger}_{323}$) of the rotational barrier around the C-N bond between biphenyl and isocyanurate rings was calculated as 27.2 kcal/mol using the Eyring equation.[102–105] The racemization behaviors of **1** at 30 (blue circles) and 70 (red circles) °C were also pursued in the similar manner: $k_{303} = 1.00 \times 10^{-7}$ sec^{-1}, $\tau_{1/2(303)}$ = 960 h (40.0 days), $\Delta G^{\ddagger}_{303}$ = 27.5 kcal/mol, $k_{343} = 5.52 \times 10^{-6}$ sec^{-1}, $\tau_{1/2(343)}$ = 17.4 h (0.73 day), $\Delta G^{\ddagger}_{343}$ = 28.4 kcal/mol. Herein, because the racemization rate at 70 °C was relatively fast, the plot data over 0–10 h were used. The $\Delta G^{\ddagger}$s calculated with the k_Ts at 30 and 70 °C was similar to that at 50 °C (see footnote[2]). Racemization of **1** is considered to arise from the rotation around the C-N bond between the biphenyl group and the isocyanurate ring at 30–70 °C (Scheme 2).

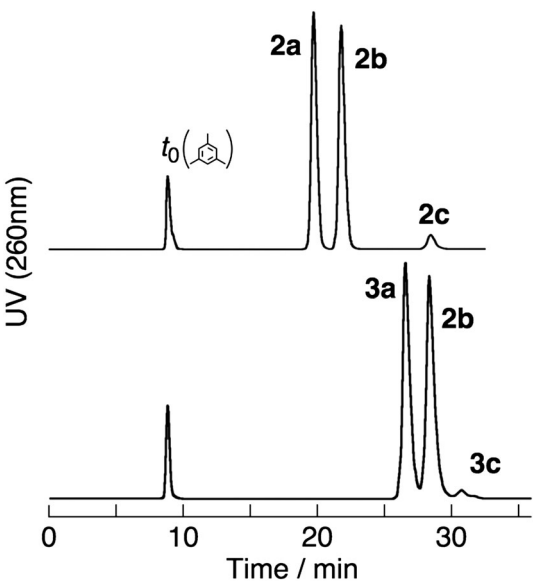

Fig. 5. Chromatographic resolution of stereoisomers of **1** on Sumichiral® OA-4600. Column: 25 × 0.46 (i.d.) cm. Eluent: hexane/ethanol/trifluoroacetic acid (90/10/0.5, v/v/v). Flow rate: 0.35 ml/min.

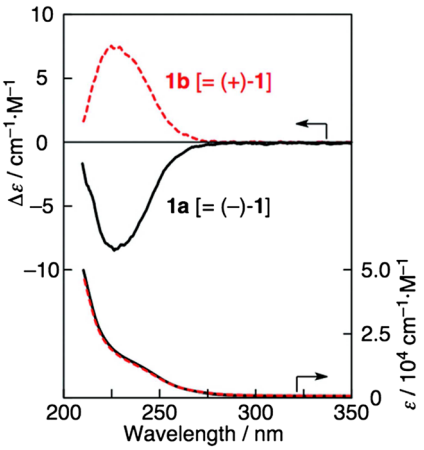

Fig. 6. Circular dichroism and absorption spectra of stereoisomers of **1** (solid line, **1a**; dashed line, **1b**) in THF at room temperature (25–27 °C). [**1**] = 0.18 mM.

Designs and Syntheses of 2 and 3

For the purpose of developing more stable isocyanurates with planar chirality than **1**, the rotation of the C-N bond must be restricted. Two strategies were worked out: (1) introduction of a bulky substituent at ortho position of Ph[1] and (2) intramolecular bridging between two benzene rings (Ph[1] and Ph[2]) adjacent to the isocyanurate ring of **1** (Scheme 3A and D). In the first strategy, although a clockwise rotation of the 2′-biphenyl group of the *anti*-form around the C-N bond induces the formation of the *syn*-form, an anti-clockwise rotation may be prevented by steric repulsion between Ph[3] and the bulky group located at ortho positions of Ph[1]. Herein, *clockwise rotation* is denoted as a rotation of the 2′-biphenyl group into the right side as shown in Scheme 3A. Another phenyl group as the bulky group was attached at the ortho position of Ph[1] of **1** to design **2** with two biphenyl groups (Fig. 3). This is because **2** adopts three structures [two

[2]The kinetic parameters ($\Delta H^{\ddagger}$ and $\Delta S^{\ddagger}$) of **1** with the racemization rates at 30, 50, and 70 °C were calculated to be 20.3 kcal/mol and −23 cal/(mol·K), respectively. Furthermore, the racemization barrier at 25 °C was estimated to be 27.2 kcal/mol with these values.

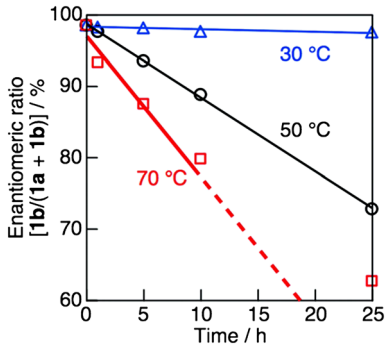

Fig. 7. Racemization behaviors of **1** at 30 (triangle), 50 (circle), and 70 °C (square) in hexane/ethanol (9/1, v/v). The enantiomeric ratio of **1b** means the ratio of the area of **1b** to that of all peaks [[area of **1b**] / [[area of **1a**] + [area of **1b**]]]. The solid lines are calculated from plot data over 0–25 (for 30 and 50 °C) or 0–10 h (for 70 °C) at each temperature using the first-order rate equation. The broken lines are extrapolated from plot data over 0–10 h at 70 °C.

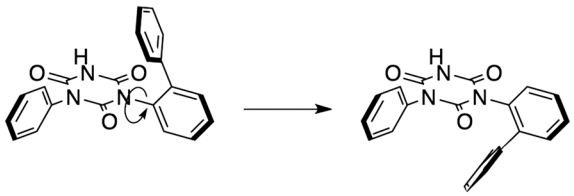

Scheme 2. Pathway of racemization of **1** at first step.

anti-forms and one syn-form (meso-form)], whereas isocyanurates with other substituents instead of the phenyl group form four structures (two anti-forms and two syn-forms). The anti-form of **2** is denoted as a stereoisomer of **2** with two phenyl groups being spatially distant from each other. The second is frequently utilized to gain representative chiral cyclophanes with planar chiralities. Even if the 2′-biphenyl group of isocyanurates intramolecularly bridged with a short spacer rotates around the C-N bond clockwise or anti-clockwise, the spacer may collide with the isocyanurate plane to inhibit the isomerization. Hexylene-1,6-dioxy group as the intramolecular bridge was employed, where the chain length was considered to be enough to restrict the rotation of the C-N bond of **3** based on molecular minimizations. The anti-form of **3** is denoted as a stereoisomer of **3** with two ethereal O atoms being spatially distant from each other.

2 was synthesized similarly to **1** (Scheme 4), whereas a different synthetic route for **3** was employed (Scheme 5) (see footnote[3]). For the synthesis of **3**, an amide **7** obtained according to the literature[97] was converted into the corresponding aniline **8** under an alkaline condition. The aniline **8** was reacted with 2-methoxyphenyl isocyanurate to afford the corresponding urea **9**. Two methoxy groups (O-CH_3) of **9** were converted into boronate groups (O-BBr_2) with boron tribromide (BBr_3), and then, the boronate groups were hydrolyzed with H_2O to generate a phenolic urea **10**. The phenolic **10** was mixed with 1,6-dibromohexane under very low concentration (<1 mM) condition to yield a cyclic urea **11**. A condensation of **11** with ethyl *N*-carbonylcarbamate[98] caused a production of **3** with the intramolecular bridging unit.[100,101]

Single crystals of **2** were obtained from a solution of **2** in hot ethanol. The ball-and-stick drawing and packing of the crystal structure of **2** are drawn in Figs. 8 and S2 in the Supporting Information, respectively. The anti-conformer of **2** ($\mathbf{2}_{anti}$) was crystallized in a monoclinic system with a space group of $P2_1/c$. Two phenyl groups in the biphenyl groups of **2** lay above and below the isocyanurate ring. Two independent molecules were *pR*- and *pS*-forms of $\mathbf{2}_{anti}$ in a unit cell. In contrast with the torsion angles for $\mathbf{2}_{anti}$ ($\phi = 78.5$ and 90.8°, $\psi = 53.7$ and 106.4°) similar to those for **1**, the spatial distances for $\mathbf{2}_{anti}$ ($d = 3.96$ and 4.76 Å) were longer than those for **1**. On the other hand, the syn-conformer of **3** ($\mathbf{3}_{syn}$) was crystallized, of which the *strap* unit blocks one face of the isocyanurate plane for $\mathbf{3}_{syn}$ (see footnote[4]). These structures were the same as those expected. Any crystals consisted of 1:1 mixtures of the antipodes.

Optical Resolutions and Isomerizations of 2 and 3

Optical resolutions of **2** and **3** were carried out by chiral HPLC under the almost same condition as that of **1** (Fig. 9). The chromatogram of **2** showed three peaks in 19.8 (first), 21.9 (second), and 28.5 (third) min; the areas of two peaks (first and second) were comparable, whereas the area of the third peak was smaller than others. Absorption (Fig. 10, bottom), ^{1}H NMR, and MS spectra of the component assignable to the first fraction (**2a**) collected by using chiral HPLC were identical with those of the second fraction (**2b**). On the other hand, a CD spectrum of **2a** exhibited a negative Cotton effect at 230 nm, whereas that of **2b** showed a positive Cotton effect (Fig. 10). These CD patterns were completely mirror images. On the contrary, the component assignable to the third fraction (**2c**) was CD-silent. In addition, although the MS spectrum of **2c** was identical with that of **2a**, the absorption and NMR spectra of **2c** were different from those of **2a**. Furthermore, the optical rotations of **2a** and **2b** were estimated to be −141 and +146, respectively. These results suggest that **2a** and **2b** are a pair of enantiomers of the anti-conformers of **2** [**2a** = (−)-$\mathbf{2}_{anti}$ and **2b** = (+)-$\mathbf{2}_{anti}$], and **2c** is the syn-conformer (meso-isomer) [**2c** = $\mathbf{2}_{syn}$] (see footnote[5]).

3 was also separated into three components [first fraction, **3a** (26.7 min); second fraction, **3b** (28.5 min); third fraction, **3c** (30.9 min)] by using chiral HPLC; the peak areas derived from **3a** and **3b** were comparable, whereas the area of **3c** was smaller than others. Absorption ($\lambda_{max} = 277$ nm, Fig. 10, bottom), ^{1}H NMR, and MS spectra of **3a** were identical with those of **3b**. On the other hand, **3a** and **3b** exhibited CD spectra with negative and positive Cotton effects at 220 nm, respectively (Fig. 10), of which patterns were mirror images. In contrast, **3c** was CD-silent. Furthermore, although the MS spectrum of **3c** was identical with that of **3a**, the absorption ($\lambda_{max} = 292$ nm) and NMR spectra of **3c** were different from

[3]Before a synthetic route of **3** as described in Scheme 5 was chosen, we carried out an alkylation of an isocyanurate bearing a phenolic hydroxy group according to the same method as those of **1** and **2**. When the isocyanurate was reacted with 1-bromohexane under basic condition, the alkylation at both phenolic oxygen and isocyanuric N atoms were observed. This result indicated that the synthetic route of **1** and **2** was unsuitable for the preparation of **3**.

[4]**3** was confirmed to form a chiral syn-form, although the quality of the crystal is not good.

[5]To investigate which of $\mathbf{2}_{syn}$ and $\mathbf{2}_{anti}$ is more stable, the geometry optimizations of $\mathbf{2}_{syn}$ and $\mathbf{2}_{anti}$ were performed using the DMol3 module as implemented in the Materials Studio software (version 5.0; Accerlys Inc. (San Diego, CA, USA)) (Figure S3 in the Supporting Information). The differential energy of $\mathbf{2}_{syn}$ against $\mathbf{2}_{anti}$ was + 2.7 kcal/mol, indicating $\mathbf{2}_{anti}$ is more stable than $\mathbf{2}_{syn}$. The value of the differential energy is consistent with the free energy (+ 1.9 kcal/mol) from the equilibrium constant based on the peak areas of three stereoisomers of **2** [[area of $\mathbf{2}_{anti}$] : [area of $\mathbf{2}_{syn}$] = 96 : 4, 298 K].

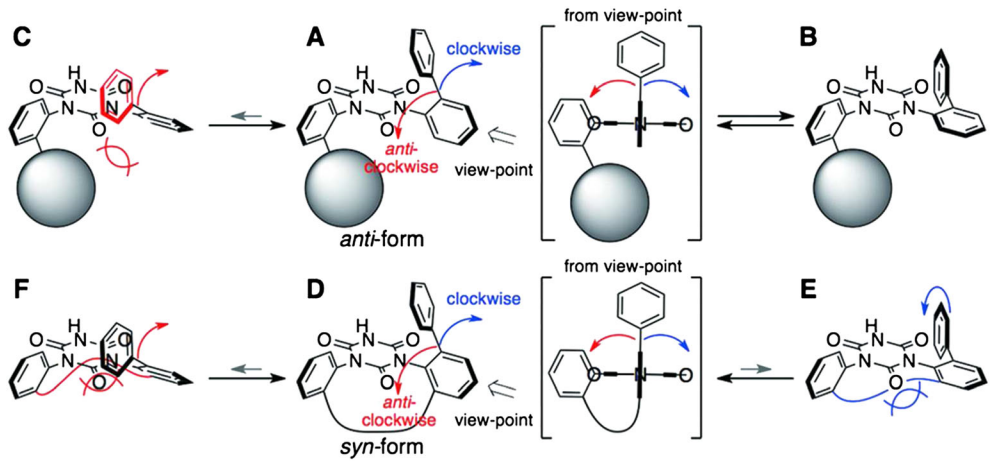

Scheme 3. Pathways to inhibit isomerizations of isocyanurates with bulky group (**A–C**) and intramolecular bridge (**D–F**).

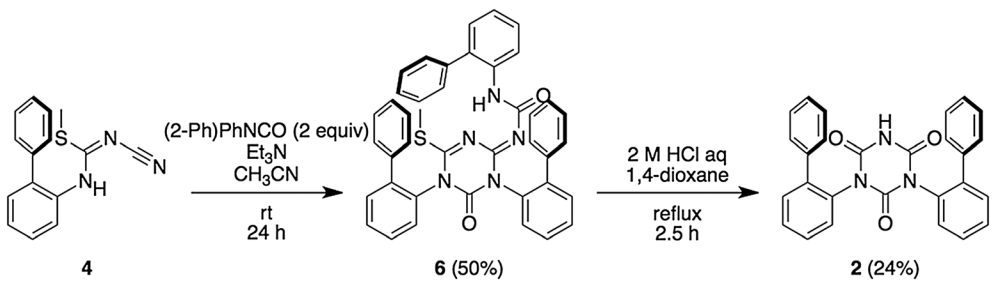

Scheme 4. Synthesis of **2**.

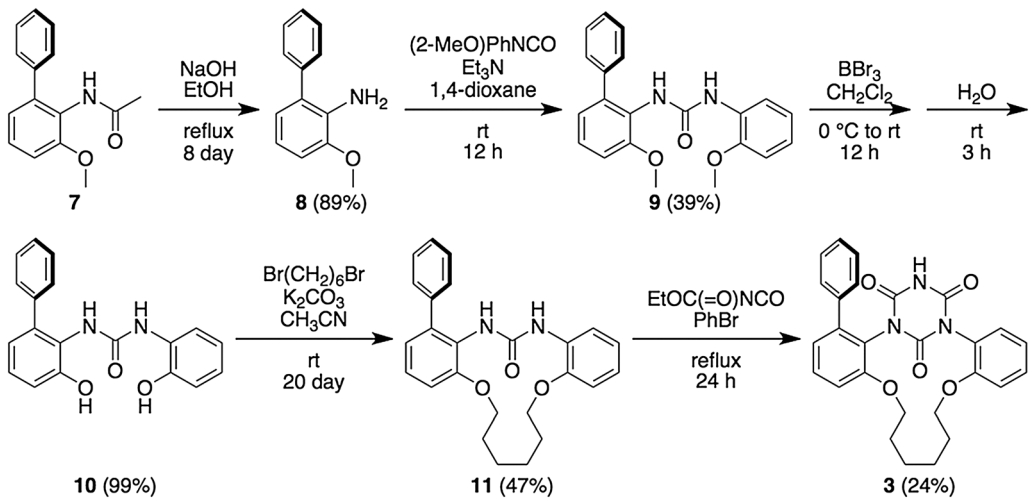

Scheme 5. Synthesis of **3**.

those of **3a**. Furthermore, the optical rotations of **3a** and **3b** were estimated to be −126 and +127, respectively. These results indicate that **3a** and **3b** are a pair of enantiomers of the syn-conformers of **3** [**3a** = (−)-$\mathbf{3}_{anti}$ and **3b** = (+)-$\mathbf{3}_{syn}$], and **3c** is a racemic mixture of the anti-conformers [**3c** = (±)-$\mathbf{3}_{anti}$] (see footnote[6]).

[6]To investigate which of $\mathbf{3}_{syn}$ and $\mathbf{3}_{anti}$ is more stable, the geometry optimizations of $\mathbf{3}_{syn}$ and $\mathbf{3}_{anti}$ were performed in the same manner as those of **2** (Fig. S3 in the Supporting Information). The differential energy of $\mathbf{3}_{anti}$ against $\mathbf{3}_{syn}$ was + 31.3 kcal/mol, indicating $\mathbf{3}_{syn}$ afforded by recrystallization is more stable than $\mathbf{3}_{anti}$.

To investigate isomerizations of **2** and **3** in solution, solutions of the isolated enantiomers **2a** (>99% ee) and **3a** (>99% ee) in hexane/ethanol (9/1, v/v) were kept at 50 and 150 °C, respectively, and then analyzed by the chiral HPLC. Whereas the peak area of **2a** decreased gradually, the peak area derived from **2c** gradually increased, followed by a slower increase of that derived from **2b** (Fig. S4). The kinetic parameters (k_{323}, $\tau_{1/2(323)}$, and $\Delta G^{\ddagger}_{323}$) of **2** were estimated to be 1.35×10^{-6} sec^{-1}, 71.5 h (2.98 days), and 27.6 kcal/mol, respectively. On the other hand, even when the solution of **3a** was kept at

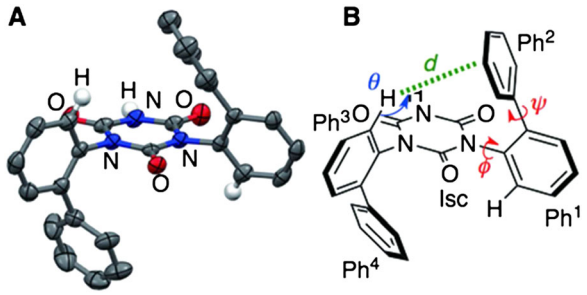

Fig. 8. Ball-and-stick drawing of $\mathbf{2}_{anti}$ with thermal ellipsoids at 50% probability. Each one of the independent molecules is shown here. H atoms are partially omitted for clarity. (**B**) Steric illustration of $\mathbf{2}_{anti}$ with denotation of benzene and heterocyclic rings, dihedral angles, spatial distance, and angle: Ph^1, Ph^2, Ph^3, Ph^4 for four benzene rings; Isc for isocyanurate ring; ϕ, χ for two dihedral angles; d for spatial distance between carbon of Ph^2 and hydrogen at ortho position of Ph^3; for angle of C-H(Ph^3)···C(Ph^2).

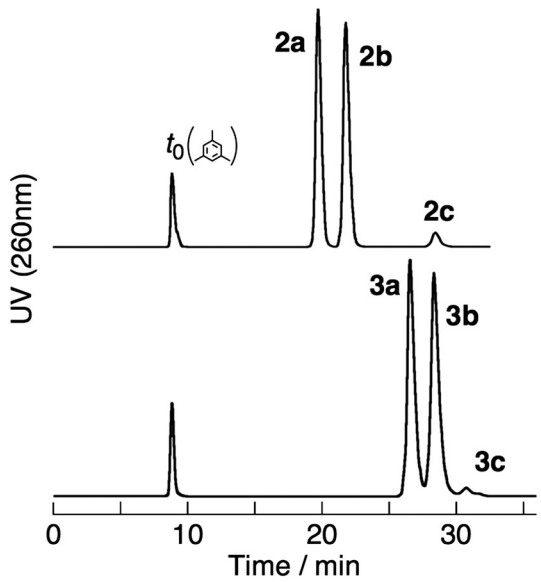

Fig. 9. Chromatographic resolutions of stereoisomers of **2** and **3** on Sumichiral® OA-4600. Column: 25 × 0.46 (i.d.) cm. Eluent: hexane/ethanol/trifluoroacetic acid (90/10/0.5, v/v/v). Flow rate: 0.35 ml/min.

150 °C for 6 days in a sealed tube, no decrease of the peak area of **3a** was observed. If a small amount (0.5 mol%) of **3a** isomerized under that condition, k_{423}, $\tau_{1/2(423)}$, and $\Delta G^{\ddagger}_{423}$ of **3** were calculated to be $<1.0 \times 10^{-8}\,sec^{-1}$, $>1.0\ 10^{4}$ h (400 days), and >40.6 kcal/mol, respectively. The lower isomerization rates of **2** and **3** than that of **1** and, in particular, the lowest rate of **3** among them were predictable results (Scheme 6), indicating that the introduction of bulky substitutes and the intramolecular bridging are effective for inhibition of isomerization.

CONCLUSIONS

The present study demonstrated a novel design of planar-chiral molecules consisting of rigid backbones such as isocyanurates. This concept is based on differentiating enantiotopic faces of C_s-symmetric rigid backbones by a perpendicular array of substituents directly connected to the backbones. Optical resolutions of the designed isocyanurates were accomplished by means of a common chiral HPLC technique. Furthermore, isomerization of the isocyanurates derived from rotational behavior around $C_{biphenyl}$-N bond was efficiently inhibited by introducing bulky groups or by intramolecular bridging. This result encourages designs of planar-chiral

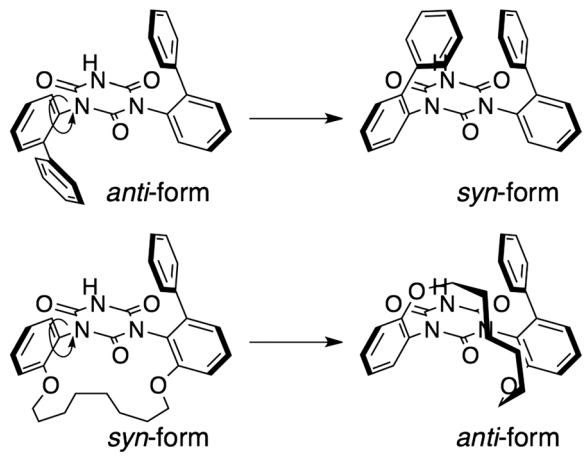

Scheme 6. Pathways of isomerizations of **2** and **3** at first steps.

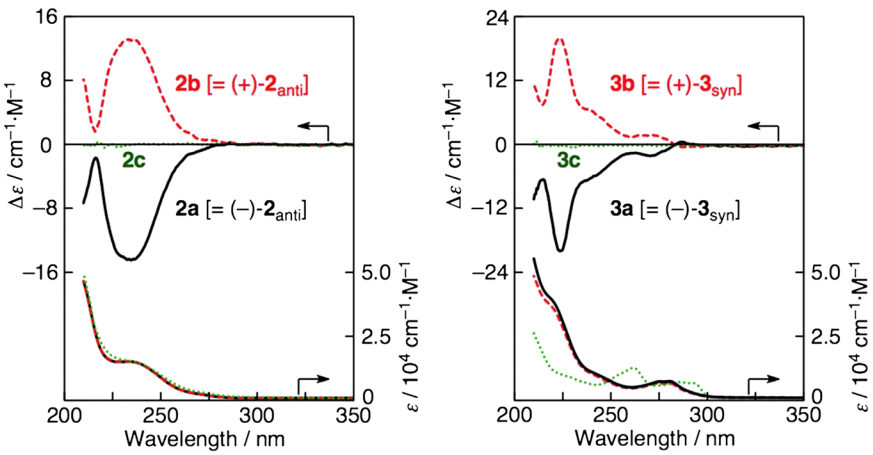

Fig. 10. Circular dichroism and absorption spectra of stereoisomers of **2** (left) and **3** (right) (solid lines, **2a** and **3a**; dashed lines, **2b** and **3b**; dotted lines, **2c** and **3c**) in THF at room temperature (25–27 °C). [**2**] = 0.14 mM, [**3**] = 0.13 mM.

molecules based on not only isocyanurates[78–95] but also C_3-symmetric molecules such as mesitylene[112–117] for asymmetric syntheses and molecular recognitions. Investigations on absolute configurations of the isocyanurates are under investigation in our laboratory.

ACKNOWLEDGMENTS

We acknowledge S. Kawaji and T. Sawada (Tokyo University of Science) for their help in the single X-ray analysis.

LITERATURE CITED

1. König B. Carbon rich cyclophanes with universal properties—an update. Top Curr Chem 1998;196:91–136.
2. Gleiter R, Hopf H, editors. *Modern cyclophane chemistry*. Weinheim: Wiley-VCH; 2004.
3. Campbell K, Tykwinski RR. Chiral carbon-rich macrocycles and cyclophanes. In: Haley MM, Tykwinski RR, editors. *Carbon-rich compounds: from molecules to materials*. Weinheim: Wiley-VCH; 2006. p 229–294.
4. Rowlands GJ. The synthesis of enantiomerically pure [2.2]paracyclophane derivatives. Org Biomol Chem 2008;6:1527–1534.
5. Aly AA, Brown AB. Asymmetric and fused heterocycles based on [2.2] paracyclophane. Tetrahedron 2009;65:8055–8089.
6. Mori T, Inoue Y. Recent theoretical and experimental advances in the electronic circular dichroisms of planar chiral cyclophanes. Top Curr Chem 2011;298:99–128.
7. Haberhauer G. Control of planar chirality: the construction of a copper-ion-controlled chiral molecular hinge. Angew Chem Int Ed 2008;47:3635–3638.
8. Mori K, Ohmori K, Suzuki K. Hydrogen-bond control in axially chiral styrenes: selective synthesis of enantiomerically pure C_2-symmetric paracyclophanes. Angew Chem Int Ed 2009;48:5638–5641.
9. Tomooka K, Ezawa T, Inoue H, Uehara K, Igawa K. Dynamic chirality of (*E*)-5-cyclononen-1-one and its enolate. J Am Chem Soc 2011;133:1754–1756.
10. Togni A, Hayashi T, editors. *Ferrocenes: homogeneous catalysis, organic synthesis, materials science*. Weinheim: VCH; 1995.
11. Stepnicka P, editor. *Ferrocenes: ligands, materials and biomolecules*. West Sussex: John-Wiley and Sons; 2008.
12. Dai LX, Hou XL, editors. *Chiral ferrocenes in asymmetric catalysis: synthesis and applications*. Weinheim: Wiley-VCH; 2010.
13. Muraoka T, Kinbara K, Kobayashi Y, Aida T. Light-driven open-close motion of chiral molecular scissors. J Am Chem Soc 2003;125:5612–5613.
14. Muraoka T, Kinbara K, Aida T. Mechanical twisting of a guest by a photoresponsive host. Nature 2006;440:512–515.
15. Gibson SE, Knight JD. [2.2]Paracyclophane derivatives in asymmetric catalysis. Org Biomol Chem 2003;1:1256–1269.
16. Kanomata N, Nakata T. A compact chemical miniature of a holoenzyme, coenzyme NADH linked dehydrogenase: design and synthesis of bridged NADH models and their highly enantioselective reduction. J Am Chem Soc 2000;122:4563–4568.
17. Gibson SE, Knight JD. Novel multichiral diols and diamines by highly stereoselective pinacol coupling of planar chiral [2.2]paracyclophane derivatives. Chem Eur J 2005;11:6944–6961.
18. Matsuoka Y, Ishida Y, Sasaki D, Saigo K. Cyclophane-type imidazolium salts with planar chirality as a new class of *N*-heterocyclic carbene precursors. Chem Eur J 2008;14:9215–9222.
19. Maeda R, Wada T, Mori T, Kono S, Kanomata N, Inoue Y. Planar-to-planar chirality transfer in the excited state: enantiodifferentiating photoisomerization of cyclooctenes sensitized by planar-chiral paracyclophane. J Am Chem Soc 2011;133:10379–10381.
20. Fu GC. Enantioselective nucleophilic catalysis with "planar-chiral" heterocycles. Acc Chem Res 2000;33:412–420.
21. Colacot TJ. A concise update on the applications of chiral ferrocenyl phosphines in homogeneous catalysis leading to organic synthesis. Chem Rev 2003;103:3101–3118.
22. Fu GC. Applications of planar-chiral heterocycles as ligands in asymmetric catalysis. Acc Chem Res 2006;39:853–860.
23. Arrayás RG, Adrio J, Carretero JC. Recent applications of chiral ferrocene ligands in asymmetric catalysis. Angew Chem Int Ed 2006;45:7674–7715.
24. Djukic JP, Hijazi A, Flack HD, Bernardinelli G. Non-racemic (scalemic) planar-chiral five-membered metallacycles: routes, means, and pitfalls in their synthesis and characterization. Chem Soc Rev 2008;37:406–425.
25. Togni A, Halterman RL, editors. *Metallocenes: synthesis, reactivity, applications*. Weinheim: Wiley-VCH; 1998.
26. Paley RS. Enantiomerically pure planar chiral organometallic complexes via facially selective π-complexation. Chem Rev 2002;102:1493–1523.
27. Ganter C. Chiral organometallic half-sandwich complexes with defined metal configuration. Chem Soc Rev 2003;32:130–138.
28. Duthaler RO, Hafner A. Chiral titanium complexes for enantioselective addition of nucleophiles to carbonyl groups. Chem Rev 1992;92:807–832.
29. Bolm C, Muniz K. Planar chiral arene chromium(0) complexes: potential ligands for asymmetric catalysis. Chem Soc Rev 1999;28:51–59.
30. Gibson SE, Ibrahim H. Asymmetric catalysis using planar chiral arene chromium complexes. Chem Commun 2002;2465–2473.
31. Rose-Munch F, Rose E. Planar chiral (η^5-cyclohexadienyl)- and (η^6-arene)-tricarbonylmanganese complexes: synthetic routes and application. Org Biomol Chem 2011;9:4725–4735.
32. Brintzinger HH, Fischer D, Mülhaupt R, Rieger B, Waymouth RM. Stereospecific olefin polymerization with chiral metallocene catalysts. Angew Chem Int Ed Engl 1995;34:1143–1170.
33. Kuran W. *Principles of Coordination Polymerization*. West Sussex: John Wiley and Sons; 2001. p 43–245.
34. Shinkai S, Ikeda M, Sugasaki A, Takeuchi M. Positive allosteric systems designed on dynamic supramolecular scaffolds: toward switching and amplification of guest affinity and selectivity. Acc Chem Rev 2001a;34:494–503.
35. Takeuchi M, Ikeda M, Sugasaki A, Shinkai S. Molecular design of artificial molecular and ion recognition systems with allosteric guest responses. Acc Chem Rev 2001b;34:865–873.
36. Inoue S, Aida T, Konishi K. Selective synthesis with metalloporphyrin catalysts. J Mol Catal 1992;74:121–129.
37. Collman JP, Zhang X, Lee VJ, Uffelman ES, Brauman JI. Regioselective and enantioselective epoxidation catalyzed by metalloporphyrins. Science 1993;261:1404–1411.
38. Ogoshi H, Mizutani T. Multifunctional and chiral porphyrins: model receptors for chiral recognition. Acc Chem Res 1998;31:81–89.
39. Marchon JC, Ramasseul R. Chiral metalloporphyrins and their use in enantiocontrol. In: Kadish K, Smith KM, Guilard R, editors. *The porphyrin handbook*, Vol. 11. San Diego: Academic Press; 2003. p 75–132.
40. Simonneaux G, Le Maux P, Ferrand Y, Rault-Berthelot J. Asymmetric heterogeneous catalysis by metalloporphyrins. Coord Chem Rev 2006;250:2212–2221.
41. Kubo H, Aida T, Inoue S. Molecular asymmetry of an *N*-alkylporphyrin with enantiotopic faces. Resolution and spectroscopic characterizations of optical antipodes of *N*-methyletioporphyrin I. J Chem Soc Chem Commun 1988;1015–1017.
42. Konishi K, Takahata Y, Aida T, Inoue S, Kuroda R. Chiral *N*-substituted porphyrins related to heme inactivation products. First crystallographic determination of absolute stereochemistry and correlation with circular dichroism. J Am Chem Soc 1993;115:1169–1170.
43. Swanson BA, Ortiz de Montellano PR. Structure and absolute stereochemistry of the four *N*-phenylprotoporphyrin IX regioisomers isolated from phenylhydrazine-treated myoglobin. J Am Chem Soc 1991;113:8146–8153.
44. Konishi K, Sugino T, Aida T, Inoue S. Stereochemical studies on reversible metal-nitrogen transfer of alkyl and aryl groups in chiral cobalt(III) porphyrins. Relevance to the mechanism of a metabolic heme inactivation process. J Am Chem Soc 1991;113:6487–6491.
45. Konishi K, Suezaki M, Aida T. The first chiral phosphorous porphyrins with molecular asymmetry: conformation studies on porphyrin macrocycles in solution. Tetrahedron Lett 1999;40:6951–6955.
46. Konishi K, Miyazaki K, Aida T, Inoue S. Photoinduced conformational ruffling of distorted porphyrin. Optical resolution and photochemical behavior of chiral "single-armed" porphyrin complexes. J Am Chem Soc 1990;112:5639–5640.
47. Konishi K, Mori Y, Aida T, Inoue S. Conformational flexibility of metalloporphyrin skeletons as studied by racemization profiles of chiral *meso*-substituted metalloporphyrins with molecular asymmetry. Inorg Chem 1995;34:1292–1294.
48. Mizutani T, Ema T, Tomita T, Kuroda Y, Ogoshi H. Recognition of chirality and residual groups of amino acid esters using new trifunctional

chiral porphyrins with C_2 symmetry. J Chem Soc Chem Commun 1993;520–522.

49. Mizutani T, Ema T, Tomita T, Kuroda Y, Ogoshi H. Design and synthesis of a trifunctional chiral porphyrin with C_2 symmetry as a chiral recognition host for amino acid esters. J Am Chem Soc 1994;116:4240–4250.
50. Chiang LC, Konishi K, Aida T, Inoue S. Asymmetric oxidation of sulfides catalysed by an iron complex of C_2-chiral strapped porphyrin as a conceptually new P-450 model catalyst. J Chem Soc Chem Commun 1992;254–256.
51. Konishi K, Oda K, Nishida K, Aida T, Inoue S. Asymmetric epoxidation of olefins catalyzed by manganese complexes of chiral "strapped" porphyrins with diastereotopic faces. A novel strategy for stereochemical modeling of the active site of cytochrome P-450. J Am Chem Soc 1992;114:1313–1317.
52. Konishi K, Yahara K, Toshishige H, Aida T, Inoue S. A novel anion-binding chiral receptor based on a metalloporphyrin with molecular asymmetry. Highly enantioselective recognition of amino acid derivative. J Am Chem Soc 1994;116:1337–1344.
53. Ito A, Konishi K, Aida T. Free bases of chiral *N*-substituted porphyrins as catalysts for asymmetric reaction. Tetrahedron Lett 1996a;37:2585–2588.
54. Konishi K, Kimata S, Yoshida K, Tanaka M, Aida T. Recognition of the helical sense of polypeptides by a chiral metalloporphyrin receptor. Angew Chem Int Ed Engl 1996b;35:2823–2826.
55. Zheng JY, Konishi K, Aida T. Guest-selective binding of *Z*-amino acids by a strapped metalloporphyrin receptor with a hydrogen-bonding capability. Tetrahedron 1997;53:9115–9122.
56. Teraoka J, Yamamoto N, Matsumoto Y, Kyogoku Y, Sugeta H. What is the crucial factor for vibrational circular dichroism in hemoprotein ligands? J Am Chem Soc 1996;118:8875–8878.
57. Tashiro K, Konishi K, Aida T. Enantiomeric resolution of chiral metallobis(porphyrin)s: studies on rotatability of electronically coupled porphyrin ligands. Angew Chem Int Ed Engl 1997;36:856–859.
58. Tashiro K, Fujiwara T, Konishi K, Aida T. Rotational oscillation of two interlocked porphyrins in cerium bis(5,15-diarylporphyrinate) double-deckers. Chem Commun 1998;1121–1122.
59. Tashiro K, Konishi K, Aida T. Metal bisporphyrinate double-decker complexes as redox-responsive rotating modules. Studies on ligand rotation activities of the reduced and oxidized forms using chirality as a probe. J Am Chem Soc 2000;122:7921–7926.
60. Furusho Y, Kimura T, Mizuno Y, Aida T. Chirality-memory molecule: a D_2-symmetric fully substituted porphyrin as a conceptually new chirality sensor. J Am Chem Soc 1997;119:5267–5268.
61. Mizuno Y, Aida T, Yamaguchi K. Chirality-memory molecule: crystallographic and spectroscopic studies on dynamic molecular recognition events by fully substituted chiral porphyrins. J Am Chem Soc 2000;122:5278–5285.
62. Mizuno Y, Alam MA, Tsuda A, Kinbara K, Yamaguchi K, Aida T. Hermaphroditic chirality of a D_2-symmetric saddle-shaped porphyrin in multicomponent spontaneous optical resolution: inclusion cocrystals with double-helical porphyrin arrays. Angew Chem Int Ed 2006;45:3786–3790.
63. Promme P, Gleiter R, Hopf H, editors. *Photosynthetic protein complexes: a structural approach*. Weinheim: Wiley-VCH; 2008.
64. Deisenhofer J, Michel H. The photosynthetic reaction center from the purple bacterium *Rhodopseudomonas viridis*. Science 1989;245:1463–1473.
65. Amunts A, Drory O, Nelson N. The structure of a plant photosystem I supercomplex at 3.4 Å resolution. Nature 2007;447:58–63.
66. Umena Y, Kawakami K, Shen JR, Kamiya N. Crystal structure of oxygen-evolving photosystem II at a resolution of 1.9 Å. Nature 2011;473:55–61.
67. Kräutler B, Arigoni D, Golding BT, editors. *Vitamin B_{12} and B_{12}-proteins*. Weinheim: Wiley-VCH; 1998.
68. Ortiz de Montellano PR, editor. *Cytochrome P450: structure, mechanism, and biochemistry*, 3rd edn. New York: Kluwer Academic/Plenum; 2005.
69. Chida H, Yokoyama T, Kawai F, Nakazawa A, Akazaki H, Takayama Y, Hirano T, Suruga K, Satoh T, Yamada S, Kawachi R, Unzai S, Nishio T, Park SY, Oku T. Crystal structure of oxidized cytochrome c_{6A} from *Arabidopsis thaliana*. FEBS Lett 2006;580:3763–3768.
70. Gay SC, Shah MB, Talakad JC, Maekawa K, Roberts AG, Wilderman PR, Sun L, Yang JY, Huelga SC, Hong WX, Zhang Q, Stout CD, Halpert JR. Crystal structure of a cytochrome P450 2B6 genetic variant in complex with the inhibitor 4-(4-chlorophenyl)imidazole at 2.0-Å resolution. Mol Pharmacol 2010;77:529–538.
71. Traut T. *Allosteric regulatory enzymes*. New York: Springer; 2008. p 105–126.
72. Schlichting I, Berendzen J, Phillips GN Jr, Sweet RM. Crystal structure of photolysed carbonmonoxy-myoglobin. Nature 1994;371:808–812.
73. Riccio A, Vitagliano L, di Prisco G, Zagari A, Mazzarella L. The crystal structure of a tetrameric hemoglobin in a partial hemichrome state. Proc Natl Acad Sci USA 2002;99:9801–9806.
74. Goto H, Hayakawa T, Furutachi K, Sugimoto H, Inoue S. Planar-chiral metal complexes comprised of square-planar metal and achiral tetradentate ligands: design, optical resolution, and thermodynamics. Inorg Chem 2012;51:4134–4142.
75. Saraswathi BS, Gowda BT, Foro S, Fuess H. *N*-(4-Methylphenyl) succinimides. Acta Crystallogr 2010;E66:o390.
76. Usanmaz A. The crystal structure of 1,3,5-triphenyl-1,3,5-perhydrotriazine-2,4,6-trione (phenylisocyanurate). Acta Crystallogr 1979;B35:1117–1119.
77. Mariyatra MB, Panchanatheswaran K, Low JN, Glidewell C. Orthorhombic and monoclinic polymorphs of 1,3,5-triphenylperhydro-1,3,5-triazine-2,4,6-trione at 120 K: chains and sheets formed by C–H···π(arene) hydrogen bonds. Acta Crystallogr 2004;C60:o682–o685.
78. Seto CT, Whitesides GM. Self-assembly based on the cyanuric acid–melamine lattice. J Am Chem Soc 1990;112:6409–6411.
79. Whitesides GM, Mathias JP, Seto CT. Molecular self-assembly and nanochemistry: a chemical strategy for the synthesis of nanostructures. Science 1991;254:1312–1319.
80. Whitesides GM, Simanek EE, Mathias JP, Seto CT, Chin D, Mammem M, Dordon DM. Noncovalent synthesis: using physical-organic chemistry to make aggregates. Acc Chem Res 1995;28:37–44.
81. Lehn JM, Mascal M, DeCian A, Fischer J. Molecular recognition directed self-assembly of ordered supramolecular strands by cocrystallization of complementary molecular components. J Chem Soc Chem Commun 1990;479–480.
82. Berl V, Krische MJ, Huc J, Lehn JM, Schmutz M. Template-induced and molecular recognition directed hierarchical generation of supramolecular assemblies from molecular strands. Chem Eur J 2000;6:1938–1946.
83. Prins LJ, Huskens J, de Jong F, Timmerman P, Reinhoudt DN. Complete asymmetric induction of supramolecular chirality in a hydrogen-bonded assembly. Nature 1999;398:498–502.
84. Prins LJ, de Jong F, Timmerman P, Reinhoudt DN. An enantiomerically pure hydrogen-bonded assembly. Nature 2000;408:181–184.
85. Prins LJ, Reinhoudt DN, Timmerman P. Noncovalent synthesis using hydrogen bonding. Angew Chem Int Ed 2001a;40:2382–2426.
86. Bielejewska AG, Marjo CE, Prins LJ, Timmerman P, de Jong F, Reinhoudt DN. Thermodynamic stabilities of linear and crinkled tapes and cyclic rosettes in melamine-cyanurate assemblies: a model description. J Am Chem Soc 2001b;123:7518–7533.
87. Reinhoudt DN, Crego-Calama M. Synthesis beyond the molecule. Science 2002;295:2403–2408.
88. Yagai S, Nakajima T, Kishikawa K, Kohmoto S, Karatsu T, Kitamura A. Hierarchical organization of photoresponsive hydrogen-bonded rosettes. J Am Chem Soc 2005;127:11134–11139.
89. Yagai S, Kitamura A. Recent advances in photoresponsive supramolecular self-assemblies. Chem Soc Rev 2008;37:1520–1529.
90. Ariga K, Kunitake T. Molecular recognition at air-water and related interfaces: complementary hydrogen bonding and multisite interaction. Acc Chem Res 1998;31:371–378.
91. Kimizuka N. Self-assembly of supramolecular nanofibers. Adv Polym Sci 2008;219:1–26.
92. Rangenathan A, Pedireddi VR, Rao CNR. Hydrothermal synthesis of organic channel structures: 1:1 Hydrogen-bonded adducts of melamine with cyanuric and trithiocyanuric acids. J Am Chem Soc 1999;121:1752–1753.
93. Wessendorf F, Gnichwitz JF, Sarova GH, Hager K, Hartnagel U, Guldi DM, Hirsch A. Implementation of a Hamilton-receptor-based hydrogen-bonding motif toward a new electron donor-acceptor prototype: electron versus energy transfer. J Am Chem Soc 2007;129:16057–16071.
94. Ma M, Gong Y, Bong D. Lipid membrane adhesion and fusion driven by designed, minimally multivalent hydrogen-bonding lipids. J Am Chem Soc 2009;131:16919–16926.
95. Noh TH, Heo E, Park KH, Jung OS. Motion of an isolated water molecule within a flexible coordination cage: structural properties and catalytic effects of ionic palladium(II) complexes. J Am Chem Soc 2011;133:1236–1237.
96. Sugimoto H, Yamane Y, Inoue S. Enantiomeric discrimination by novel optically active isocyanurates having peripheral amino acid units. Tetrahedron: Asymmetry 2000;11:2067–2075.

97. Yang S, Li B, Wan X, Shi Z. Ortho arylation of acetanilides via Pd(II)-catalyzed C–H functionalization. J Am Chem Soc 2007;129:6066–6067.
98. Lamon RW. Substituted uracils from ethoxycarbonyl isocyanate and primary or secondary enamines. J Heterocycl Chem 1969;6:261–264.
99. Suyama S, Kimura A, Kiuchi Y. The reaction of 3-cyano-2-methyl-1-phenylisothiourea with isocyanate, isothiocyanate, and carbodiimide. Nippon Kagaku Kaishi 1996;845–848 (in Japanese).
100. Badawey ESAM, Hassan AMM, Kappe T. Synthesis of new benzimidazole derivatives as potential antimicrobial agents. Arch Pharm 1991;324:355–357.
101. Guo ZQ, Wu DP, Zhu YF, Tucci FC, Pontillo J, Saunders J, Xie Q, Struthers RS, Chen C. A convenient one-pot synthesis of asymmetric 1,3,5-triazine-2,4,6-triones and its application towards a novel class of gonadotropin-releasing hormone receptor antagonists. Bioorg Med Chem Lett 2005;15:693–698.
102. Cagle FW, Eyring H. Application of absolute reaction rate theory to the racemization of certain sterically hindered compounds. J Am Chem Soc 1951;73:5628–5630.
103. Trapp O, Trapp G, Kong JW, Hahn U, Vögtle F, Schurig V. Probing the stereointegrity of Tröger's base—a dynamic electrokinetic chromatographic study. Chem Eur J 2002;8:3629–3634.
104. Osswald P, Würthner F. Effects of bay substituents on the racemization barriers of perylene bisimides: resolution of atropo-enantiomers. J Am Chem Soc 2007;129:14319–14326.
105. Wolf C. *Dynamic stereochemistry of chiral compounds*. Cambridge: Royal Society of Chemistry; 2008. p 136–179.
106. Clews CJB, Lonsdale K. Structure of 1,2-diphenylbenzene ($C_{18}H_{14}$). Proc R Soc Lond A 1937;161:493–504.
107. Aikawa S, Maruyama Y, Ohashi Y, Sasada Y. 1,2-Diphenylbenzene (*o*-terphenyl). Acta Crystallogr 1978;B34:2901–2904.
108. George M, Brown M, Levy HA. *o*-Terphenyl by neutron diffraction. Acta Crystallogr 1979;B35:785–788.
109. Sugimoto H, Aida T, Inoue S. Unusual conformational stability of a sterically crowded atropisomer of methyl[α^4-5,10,15,20-tetrakis(2′-phenylphenyl) porphyrinato]aluminum: a possibility of CH–π bonding interactions in organometallic porphyrin systems. J Chem Soc Chem Commun 1995;1411–1412.
110. Nishio M, Hirota M, Umezawa Y. *The CH/π interaction: evidence, nature, and consequences*. New York: Wiley-VCH; 1998.
111. Nishio M, Umezawa Y. The CH/π hydrogen bond: an important molecular force in controlling the crystal conformation of organic compounds and three-dimensional structure of biopolymers. Top Stereochem 2006;25:255–302.
112. Moberg C. C_3 symmetry in asymmetric catalysis and chiral recognition. Angew Chem Int Ed 1998;37:248–268.
113. Ballester P, Capó M, Costa A, Deya PM, Gomila R, Decken A, Deslongchamps G. Dual binding mode of methylmethanetriacetic acid to tripodal amidopyridine receptors. J Org Chem 2002;67:8832–8841.
114. Steed JW. A modular approach to anion binding podands: adaptability in design and synthesis leads to adaptability in properties. Chem Commun 2006;2637–2649.
115. Gibson SE, Castaldi MP. Applications of chiral C_3-symmetric molecules. Chem Commun 2006;3045–3062.
116. Jiang X, Lim YK, Zhang BJ, Opsitnick EA, Baik MH, Lee D. Dendritic molecular switch: chiral folding and helicity inversion. J Am Chem Soc 2008;130:16812–16822.
117. Mercer DJ, Loeb SJ. Metal-based anion receptors: an application of second-sphere coordination. Chem Soc Rev 2010;39:3612–3620.
118. Aida T, Inoue S. Metalloporphyrins as catalysts for precision macromolecular synthesis. In: Kadish KM, Smith KM, Guilard R, editors. *The porphyrin handbook*, vol. 6. San Diego: Academic Press; 2000. p 133–156.